153-7730

FINAL TECHNICAL REPORT

NAG1-2068

THE CONSTITUTIVE MODELING OF THIN FILMS WITH RANDOM MATERIAL WRINKLES

by

Thomas W. Murphey

and

Martin M. Mikulas

July 2001

THE CONSTITUTIVE MODELING OF THIN FILMS WITH RANDOM MATERIAL WRINKLES

Thomas W. Murphey*
Martin M. Mikulas**

Abstract

Material wrinkles drastically alter the structural constitutive properties of thin films. Normally linear elastic materials, when wrinkled, become highly nonlinear and initially inelastic. Stiffness' reduced by 99% and negative Poisson's ratios are typically observed. This paper presents an effective continuum constitutive model for the elastic effects of material wrinkles in thin films. The model considers general two-dimensional stress and strain states (simultaneous bi-axial and shear stress/strain) and neglects out of plane bending. The constitutive model is derived from a traditional mechanics analysis of an idealized physical model of random material wrinkles. Model parameters are the directly measurable wrinkle characteristics of amplitude and wavelength. For these reasons, the equations are mechanistic and deterministic. The model is compared with bi-axial tensile test data for wrinkled Kapton® HN and is shown to deterministically predict strain as a function of stress with an average RMS error of 22%. On average, fitting the model to test data yields an RMS error of 1.2%

Introduction

Thin films are increasingly used as structural elements of lightly stressed space structures such as sunshields, inflatable parabolic reflectors, and solar sails.[1,2] Analysis often assumes a linear behavior, however, fabrication, handling and packaging processes can induce permanent material wrinkles. These material wrinkles drastically change the thin film constitutive behavior and consequently, the shape, dynamic, and reflective characteristics of structures.

Consider a 400 in. diameter thin film reflector that requires a 0.2 in. shape accuracy and hence, a (0.2 in.)/(400 in.) = 0.0005 strain accuracy. The structure will exhibit some level of material wrinkles due to permanent creases formed in the manufacturing, packaging, and deployment processes. If these wrinkles are assumed to be spaced at 0.5 in. intervals, a wrinkle amplitude of only 0.0079 in. will cause strain errors equal to the required strain accuracy, Equation (26). Further, in a 1.0 mil thick material with $E = 10^6$ psi and $\nu = 0.3$, a 133 psi equibiaxial stress is required to remove 95% of strains due to wrinkles.† At this stress level, linear strains due to mid-plane stretching ($\varepsilon_{mid-plane} = \sigma(1-\nu)/E = 0.000093$) are much larger than strains due to wrinkles ($\varepsilon_{wrinkles} = 0.05 * 0.0005 = 0.000025$). However, at the low stress levels ($\sigma \approx 5$ psi) typical of space applications, deformations due to wrinkles (0.000144) dominate over mid-plane stretching strains (0.000004).‡ The undeformed profile of such wrinkles is shown to scale in Figure 1. The wrinkles are hardly visible; yet, they drive the structure's shape and detrimental errors result with their neglect.

Wrinkles alter the dynamic characteristics of a structure through changes in effective material stiffness properties as well. At very low stress levels, the preceding wrinkles reduce Young's modulus by 99.5% from that of the base material and induce a minimum Poisson's ratio of –0.63.§,**

The preceding predictions are made based on the constitutive model presented in this paper. While previous studies described an experimental method to measure the stiffness effects of random wrinkles, they did not fully characterize constitutive behavior nor did they enable the response of an untested material to be predicted.[3] In contrast, the constitutive model presented here is deterministic and allows preliminary constitutive behavior predictions to be made without tensile testing.

The model is a two-dimensional effective continuum representation of random material wrinkles and is derived from a traditional mechanics analysis of an idealized physical model of wrinkles. Base material mid-plane stretching and global out-of-plane bending are neglected. Toward this end, wrinkled thin film deformation terminology and mechanisms are first

* Research Engineer, Air Force Research Lab
** Professor Emeritus, University of Colorado, Boulder, Colorado, AIAA Fellow

† Eq. (22) with $\bar{\varepsilon}_j = -0.05$ gives $\alpha = 40.5$, Eq. (10) gives $\sigma_{cr} = 3.29$ psi and from Eq. (8), $\sigma = 133$ psi.

‡ From Eq. (22), with $\varepsilon_o = 0.0005$ and $\alpha = 1.52$.

§ From Eq. (24), $E_o = 5334$ psi.

** Eq. (25) evaluated at $\alpha_1 = 0$ and $\alpha_2 = 23.2$, gives $\nu_{wrinkles} = -0.93$ so that $\nu_{total} = -0.93 + 0.3 = -0.63$.

reviewed and then the model is derived. Lastly, test results demonstrating the deterministic qualities of the model are presented.

Wrinkle Terminology

Material wrinkles are permanent out-of-plane deformations caused by yielding of a material when it is folded in a tight radius or creased. Material wrinkles remain after loads are removed. In contrast, *structural wrinkles* are regions of temporary elastic buckling caused by compressive membrane stresses. Structural wrinkles disappear when loads are removed. Only material wrinkles are considered here.

Figure 2 illustrates two classes of material wrinkles, *random* and *systematic*. Random wrinkles are caused by uniformly crushing a thin film. They are effectively homogeneous and directionally independent at scales much larger than a single wrinkle. Systematic material wrinkles are those generated by folding or otherwise creasing a thin film in a specific, repeating pattern. Although systematic wrinkle patterns may exist that result in constitutive behaviors similar to random wrinkles, they are generally different. Fundamentally, the directional dependence of systematic wrinkles gives rise to a material orientation dependence. Only random material wrinkles are considered here.

Wrinkled thin film deformations may be either elastic or plastic. Consider a thin film that is crushed into a small ball to induce random wrinkles as shown in Figure 3a. This state corresponds to a thin film structure that is packaged for transportation. As shown in Figure 3b, the film does not expand to any resemblance of a flat surface when compressive loads are removed. Rather, it retains a shape closer to that of the compressed ball. This behavior is a result of plastic deformations that have occurred in the crushing process. In this ball-like state, the material will exhibit an elastic behavior only for very small applied loads. Application of larger loads (Figure 3c) will cause reverse plastic deformations in the vicinity of creases and permanently decrease wrinkle amplitudes. As wrinkles are reduced by higher stresses, the material will no longer return to a ball-like shape; a plastic response is observed. With adequate loads, enough wrinkles are removed and a sample can be considered flat at scales much larger than a single wrinkle (Figure 3d). In this quasi-flat state, loads up to the maximum applied stress will result in only elastic deformations. The material will follow the elastic response curve.

Two constitutive behavior problems are apparent with the deployment and operation of thin film structures. First, there is the plasticity problem of characterizing material behavior as it is stretched out from a packaged shape to an operational shape. Second, there is the problem of characterizing material behavior in the operational state. In this paper, the hyperelastic behavior of randomly wrinkled thin films in the operational state is considered.

Deformation Mechanisms

The dominant deformation mechanism in wrinkled thin films, bending, is revealed through the concept of a *developable surface*. A developable surface is one that can be formed from a flat plane through only bending; extensional or mid-plane stretching is not allowed.[4] Wrinkled thin films begin as flat planes, are wrinkled by material bending, and can be returned to a flat plane through only material bending.

This bending mechanism enables a qualitative description of the uniaxial constitutive behavior of wrinkled thin films. At low stress levels, bending allows the material to be highly compliant. Small changes in stress cause large changes in strain as wrinkles easily pull out. When wrinkles are mostly pulled out, the bending deformation mechanism no longer exists. The stressed material is much stiffer because it can only deform through mid-plane stretching governed by Hooke's law.

Deformations in the direction transverse to the load are described by a kinematic mechanism. In contrast to typical engineering materials, wrinkled thin films expand in both the axial and transverse directions when subjected to a uniaxial stress; Poisson's ratio is negative. This is a kinematic consequence of the bending deformations associated with the expansion of wrinkles not parallel to the load direction. A uniaxial stress will pull out all wrinkles that are not exactly parallel to the load axis. Because wrinkles expand perpendicular to their axis, the expansion of an off-axis wrinkle will cause positive strain components in the load direction as well as the transverse direction (Figure 4).

Requirements for Characterizing Constitutive Behavior

It will be shown that the general in-plane constitutive behavior of a preconditioned randomly wrinkled thin film is described by the single function, $\varepsilon_1(\sigma_1,\sigma_2)$, where *1* and *2* refer to the coincident principal stress and strain directions. The model is limited to scales much larger than a single wrinkle, such that the effects of individual wrinkles average out to an effective continuum behavior. The pristine or unwrinkled material is assumed to be isotropic and linearly elastic (while this assumption limits the range of materials to which the model applies, it is a mathematical requirement of the model). Within these assumptions, however, the description is general. General material deformations $(\varepsilon_x,\varepsilon_y,\gamma_{xy})$ are considered for a general stress state $(\sigma_x,\sigma_y,\tau_{xy})$.

Characterizing the general in-plane constitutive behavior of a material mathematically consists of determining the three functions, $\varepsilon_x(\sigma_x,\sigma_y,\tau_{xy})$, $\varepsilon_y(\sigma_x,\sigma_y,\tau_{xy})$ and $\gamma_{xy}(\sigma_x,\sigma_y,\tau_{xy})$. The reduction of these to the single function, $\varepsilon_1(\sigma_1,\sigma_2)$, follows from the initial isotropy, strain-induced orthotropy, and coincidence of principal stress and strain axes in randomly wrinkled thin films.

Wrinkled thin films are isotropic with respect to incrementally small deformations when wrinkle geometry is effectively symmetric about any and all planes. This occurs only under equibiaxial and zero stress conditions, where wrinkles are pulled out equally in each direction. Thus, wrinkled thin films lack an initial material directional dependence and are called *initially isotropic*. Consequently, any stress state path will result in the same deformation state (relative to the stress orientation), regardless of material orientation.

Wrinkled thin films also exhibit *strain-induced orthotropy*. Any deviation from an equibiaxial stress state causes wrinkle geometry to pull out non-uniformly. Wrinkles pull out most in the direction of the major principal stress and least in the orthogonal direction of the minor principal stress. Because wrinkle geometry remains symmetric about two orthogonal planes, the material is orthotropic and the principal stress directions always coincide with principal material directions. When principal stress directions coincide with principal material directions in orthotropic materials, a shear strain is not induced. Thus, principal stress directions always coincide with principal strain directions.

The original three strain functions ($\varepsilon_x,\varepsilon_y,\gamma_{xy}$) are reduced by considering only principal stresses and strains, as follows. Any arbitrary stress state can be expressed in terms of principal stresses (σ_1,σ_2). The principal strains are then calculated from $\varepsilon_1(\sigma_1,\sigma_2)$ and $\varepsilon_2(\sigma_1,\sigma_2)$. The principal strains are lastly transformed back to the original orientation to arrive at the general strain functions ($\varepsilon_x,\varepsilon_y,\gamma_{xy}$).

Further, due to the material orientation independence, stress and strain can be transformed by 90 deg. and the same behavior results,

$$\varepsilon_2(\sigma_1,\sigma_2)=\varepsilon_1(\sigma_2,\sigma_1). \qquad (1)$$

Thus, to determine the general in-plane constitutive behavior of a directionally independent hyperelastic material it is sufficient to characterize the single function, $\varepsilon_1(\sigma_1,\sigma_2)$. Further restricting the range of stresses, thin films are assumed to have a sufficiently low bending stiffness that they buckle when the minimum principal stress is compressive. Only tensile principal stresses are considered.

Deterministic Mechanistic Constitutive Model

The profile of a wrinkled Kapton® HN sample is shown in Figure 5. Two types of wrinkles are present: small radius creases and large radius curves. The large radius curves pull out at relatively low stress levels, leaving creases to dominate material constitutive behavior. This observation prompted the development of a physical model based on tightly creased beams as opposed to large radius curves. Illustrations of the physical model in original and deformed configurations are shown in Figure 6. The model is created from a rectangular arrangement of beams bent in the initial profile of a zigzag and connected at points of maximum distance from mid-plane. The connecting points were chosen such that straightening out one set of parallel beams has a tendency to do the same to the transverse set of beams, thus, including the negative Poisson's ratio mechanism. To control the Poisson's ratio effect, the model also includes linear springs at the beam connecting points. This allows beams in one direction to straighten out, and encourages beams in the transverse direction to also straighten out, but does not require them to do so by an equal amount.

The model is considered to represent only principal material axes. When subjected to stress states that include shear, the physical orientation of the model is not fixed. It is assumed to rotate and align with the principal axes.

The macroscopic in-plane constitutive behavior of the model, $\varepsilon_1(\sigma_1,\sigma_2)$, is derived by first analytically determining the effective extensional behavior of the smallest repeating element of the model. A geometrically nonlinear beam-column analysis is used. The model components are then mathematically assembled to arrive at the effective extensional behavior of the full model.

The natural configuration profile of the smallest model element is given by,

$$w_o = 2\frac{a_o}{l}x. \qquad (2)$$

In bending a straight beam into a zigzag profile, it is shortened by an amount (δ_o, Figure 7) approximated by,[5]

$$\delta_o = \frac{1}{2}\int_0^l \left(\frac{dw_o}{dx}\right)^2 dx = 2\frac{a_o^2}{l}. \qquad (3)$$

This leads to an effective initial shrinkage strain of,

$$\varepsilon_o = \frac{\delta_o}{L} = \frac{\delta_o}{l+\delta_o} = \frac{1}{1+\frac{1}{2}\left(\frac{l}{a_o}\right)^2}. \quad (4)$$

The initial shrinkage is a direct measurement of how much smaller the wrinkled and preconditioned material under zero stress is compared to the unwrinkled sample under zero stress. Strains are engineering strains and are based on a gage length that corresponds to the pristine material under zero stress. As a result, the strains predicted by the model are negative; wrinkles always have a tendency to effectively shrink materials.

A free-body diagram of the model repeating element is shown in Figure 8. Moments are established in the beam given by,

$$M = Pw - xQ/2. \quad (5)$$

The moment is based on the deformed profile (w) to include the geometrically nonlinear effects of large displacements. w is the profile of the beam after P and Q are applied and it is given by,

$$w = w_o + w_1, \quad (6)$$

where w_1 represents the displacements caused by P and Q that are in addition to w_o. The governing differential equation for deflection of the beam-column is,

$$\frac{\partial^2 w_1}{\partial x^2} = \frac{P}{EI}(w_o + w_1) - \frac{Q}{2EI}x. \quad (7)$$

The final constitutive model is simplified by introducing the two non-dimensional ratios α and β. α is the ratio of P to the Euler buckling load of the beam (P_{cr}) and β is the ratio of the transverse deflection (y_{max}) caused only by Q to the initial wrinkle amplitude, a_o,

$$P_{cr} = \pi^2 \frac{EI}{l^2}, \quad \alpha = \frac{\sigma}{\sigma_{cr}} = \frac{P}{P_{cr}} = \frac{Pl^2}{\pi^2 EI}, \quad (8)$$

$$y_{max} = \frac{Ql^3}{48EI}, \quad \beta = \frac{y_{max}}{a_o} = \frac{Ql^3}{48EIa_o}. \quad (9)$$

In evaluating σ_{cr}, the beam length and width are equal to the wrinkle wavelength and the beam thickness is the material thickness,

$$\sigma_{cr} = E\frac{\pi^2}{12}\left(\frac{t}{l}\right)^2. \quad (10)$$

With the non-dimensional parameters, Equation (7) becomes,

$$\frac{\partial^2 w_1}{\partial x^2} = \alpha\frac{\pi^2}{l^2}(w_o + w_1) - \beta\frac{24a_o}{l^3}x. \quad (11)$$

The boundary conditions for Equation (11) are $w_1 = 0$ at $x = 0$ and $w_1' = 0$ at $x = l/2$, resulting in the solution,

$$w = w_o + w_1 = \frac{2a_o}{\pi^3\alpha^{3/2}l}\left[12\pi x\beta\sqrt{\alpha} + l(\alpha\pi^2 - 12\beta)\operatorname{sech}\left(\frac{\pi}{2}\sqrt{\alpha}\right)\sinh\left(x\frac{\pi}{l}\sqrt{\alpha}\right)\right]. \quad (12)$$

The ratio of the loaded beam amplitude to the original beam amplitude, at the coupling spring connection point ($x = l/2$) is,

$$\bar{a} = \left.\frac{w}{a_o}\right|_{x=l/2} = \frac{2}{\pi^3\alpha^{3/2}}\left[6\pi\beta\sqrt{\alpha} + (\pi^2\alpha - 12\beta)\tanh\left(\frac{\pi}{2}\sqrt{\alpha}\right)\right]. \quad (13)$$

The total shortening (δ) of the beam-column, due to initial bending and application of loads, is approximated using,[6]

$$\delta = 2\int_0^{l/2}\left(\frac{dw}{dx}\right)^2 dx. \quad (14)$$

This leads to the one-dimensional creased beam-column constitutive equation,

$$\bar{\varepsilon} = \frac{\varepsilon}{\varepsilon_o} = \frac{-\delta/L}{\varepsilon_o} = \frac{-\operatorname{sech}\left(\frac{\pi}{2}\sqrt{\alpha}\right)^2}{2\pi^5\alpha^{5/2}} \left\{\pi\sqrt{\alpha}\left[\pi^4\alpha^2 - 24\pi^2\alpha\beta + 288\beta^2 + 144\beta^2\cosh\left(\pi\sqrt{\alpha}\right)\right] + (\pi^2\alpha - 12\beta)(\pi^2\alpha + 36\beta)\sinh\left(\pi\sqrt{\alpha}\right)\right\}. \quad (15)$$

Equations (13) and (15) are used to formulate the behavior of the unit cell of Figure 9. This is the smallest unit that fully captures the behavior of the model. A linear spring of non-dimensional stiffness κ is used as a first order approximation of the mechanism coupling axial and transverse strains. The spring does not structurally represent an identified deformation mechanism; it mimics behavior observed in test data. Normally, such a caveat would prevent a model from being deterministic. Hower, it has been observed that κ typically takes a value close to 0.5 and this value is assumed in the model. It is also assumed that there is a elusive structural explanation that justifies the assumption.

A force balance on the two beam-columns of the unit cell results in the following two equations for transverse loads,

$$\beta_1 = \kappa(\bar{a}_2 - \bar{a}_1) \text{ and } \beta_2 = -\beta_1, \quad (16)$$

where,

$$\bar{a}_1 = \frac{a_1}{a_0} \text{ and } \bar{a}_2 = \frac{a_2}{a_0}. \quad (17)$$

Subscripts *1* and *2* refer to the model beam and principal stress/strain directions. κ is the ratio of the linear spring stiffness (k) to the effective linear transverse stiffness of the beam ($k_{effective} = 48EI/l^3$),

$$\kappa = \frac{k}{k_{effective}} = \frac{kl^3}{48EI}. \quad (18)$$

Equations (16) are two equations in β_1 and β_2 with solution,

$$\begin{aligned}\beta_1 = {} & 2\kappa\pi^2\alpha_1\alpha_2\left[-\sqrt{\alpha_2}\tanh\left(\frac{\pi}{2}\sqrt{\alpha_1}\right)\right. \\ & \left.+\sqrt{\alpha_1}\tanh\left(\frac{\pi}{2}\sqrt{\alpha_2}\right)\right] \\ & \left\{-24\kappa\alpha_2^{3/2}\tanh\left(\frac{\pi}{2}\sqrt{\alpha_1}\right)\right. \\ & +\pi\sqrt{\alpha_1\alpha_2}\left[\pi^2\alpha_1\alpha_2+12\kappa(\alpha_1+\alpha_2)\right] \\ & \left.-24\kappa\alpha_1^{3/2}\tanh\left(\frac{\pi}{2}\sqrt{\alpha_2}\right)\right\}^{-1}\end{aligned} \quad (19)$$

Substitution of Equation (19) into Equation (15) gives the final effective continuum constitutive behavior of the model,

$$\begin{aligned}\bar{\varepsilon}_1 = \frac{\varepsilon_1}{\varepsilon_o} = {} & \\ & \frac{-1}{2\pi^5\alpha_1^3}\left\{\operatorname{sech}\left(\frac{\pi}{2}\sqrt{\alpha_1}\right)^2\left[\pi\alpha_1\left(\pi^4\alpha_1^2\right.\right.\right. \\ & \left.-24\pi^2\alpha_1\beta_1+288\beta_1^2+144\beta_1^2\cosh\left(\pi\sqrt{\alpha_1}\right)\right) \\ & \left.\left.+\sqrt{\alpha_1}\left(\pi^2\alpha_1-12\beta_1\right)\left(\pi^2\alpha_1+36\beta_1\right)\sinh\left(\pi\sqrt{\alpha_1}\right)\right]\right\}\end{aligned} \quad (20)$$

where, if $\kappa = 1/2$ is assumed,

$$\begin{aligned}\beta_1 = {} & \pi^2\alpha_1\alpha_2\left[-\sqrt{\alpha_2}\tanh\left(\frac{\pi}{2}\sqrt{\alpha_1}\right)+\sqrt{\alpha_1}\tanh\left(\frac{\pi}{2}\sqrt{\alpha_2}\right)\right] \\ & \left\{\sqrt{\alpha_1}\left[\pi\sqrt{\alpha_2}\left(\pi^2\alpha_1\alpha_2+6(\alpha_1+\alpha_2)\right)\right.\right. \\ & \left.\left.-12\alpha_1\tanh\left(\frac{\pi}{2}\sqrt{\alpha_2}\right)\right]-12\alpha_2^{3/2}\tanh\left(\frac{\pi}{2}\sqrt{\alpha_1}\right)\right\}^{-1}\end{aligned} \quad (21)$$

Equation (20) is graphed in Figure 10. For the special case of equibiaxial stress ($\alpha = \alpha_1 = \alpha_2$), the model reduces to,

$$\bar{\varepsilon} = -\frac{1}{2\pi\sqrt{\alpha}}\operatorname{sech}\left(\frac{\pi}{2}\sqrt{\alpha}\right)^2\left(\pi\sqrt{\alpha}+\sinh\left(\pi\sqrt{\alpha}\right)\right). \quad (22)$$

Total strains are the sum of strains due to bending, Equation (20), and strains due to mid-plane stretching,

$$\begin{aligned}\varepsilon_1^{total} &= \varepsilon_1 + \varepsilon_1^{mid-plane} \\ \varepsilon_1^{mid-plane} &= \frac{1}{E}\left(\sigma_1 - \nu\sigma_2\right)\end{aligned}. \quad (23)$$

Initial Stiffness

The model reveals a surprisingly simple expression for the initial (near zero stress) effective Young's modulus,

$$E_o = \left(\left.\frac{\partial\varepsilon_1}{\partial\sigma_1}\right|_{\substack{\sigma_1\to 0\\ \sigma_2\to 0}}\right)^{-1} = \frac{\sigma_{cr}}{\varepsilon_o}\left(\left.\frac{\partial\bar{\varepsilon}_1}{\partial\alpha_1}\right|_{\substack{\alpha_1\to 0\\ \alpha_2\to 0}}\right)^{-1} = \frac{\sigma_{cr}}{\varepsilon_o}\frac{8}{\pi^2}. \quad (24)$$

The effective initial Poisson's ratio turns out to be a constant, independent of specific wrinkle geometry.

$$\nu_o^{tan} = -\left.\frac{\dfrac{\partial\varepsilon_2}{\partial\sigma_1}}{\dfrac{\partial\varepsilon_1}{\partial\sigma_1}}\right|_{\substack{\sigma_1\to 0\\ \sigma_2\to 0}} = -\left.\frac{\dfrac{\partial\bar{\varepsilon}_2}{\partial\alpha_1}}{\dfrac{\partial\bar{\varepsilon}_1}{\partial\alpha_1}}\right|_{\substack{\alpha_1\to 0\\ \alpha_2\to 0}} = -\frac{1}{3}. \quad (25)$$

A minimum Poisson's ratio of –0.933 occurs when Equation (25) is evaluated at a $\alpha_2 = 23.2$.

Model Parameters

The two model parameters that vary with different randomly wrinkled thin films are ε_o and σ_{cr}. Because the model is deterministic, these parameters can be calculated directly from measurements of material microstructure characteristics: wrinkle amplitude and wavelength. To calculate wrinkle geometry from the model parameters, it is often useful to use the inverted form of Equations (4) and (10),

$$l = \pi t\sqrt{\frac{E}{12\sigma_{cr}}} \text{ and } a_o = l\frac{1}{\sqrt{2}}\sqrt{\frac{\varepsilon_o}{1-\varepsilon_o}}. \quad (26)$$

The model parameters have physical interpretations that enable intuitive comparisons of different wrinkle geometries and materials. Parameter interpretations are most perceptible for the case of equibiaxial stress, which is graphed in Figure 11 for several representative parameter values. σ_{cr} controls the relative stress level at which wrinkles pull out; a larger σ_{cr} indicates that a larger stress is required to pull wrinkles out. From Equation (10), a longer wrinkle wavelength results in a smaller σ_{cr}. Longer wavelength wrinkles pull out at lower stress levels than shorter wavelength wrinkles, regardless of wrinkle amplitude. The effect of material thickness is also evaluated purely through σ_{cr} (ε_o is not a function of material thickness). From Equation (10), decreasing material thickness decreases σ_{cr}. For constant wrinkle geometry, wrinkles pull out at a lower stress for thinner materials ($\sigma_{cr} \propto t^2$).

ε_o, which is a function of the ratio l/a_o, determines the relative magnitude of strains due to wrinkles. Due to its dependence on l and a_o, several different wrinkle geometries will result in equal initial shrinkages. Only as wrinkle amplitude decreases relative to wrinkle wavelength does the initial shrinkage also decrease.

Model Validation

The model has been observed to exhibit deterministic qualities. The constitutive behavior predicted by the model when parameters are estimated from direct measurements of wrinkle geometry correlates with the constitutive behavior observed from biaxial tensile data. This *direct method* of estimating model parameters from measurements of wrinkle geometry, however, does not yield highly accurate results. In Murphey's tests the average difference between model and test data was 22% of ε_o.[7] The results are adequate for preliminary design calculations only. A primary limitation of the direct method is in assigning a single wrinkle amplitude and wavelength that best characterize a sample with much broader wrinkle spectral content. Model predictions based on the direct measurement method of parameter estimation are compared with experimental data in Figure 12.

More accurate regression based parameter estimation techniques using tensile test data have also been investigated. The regression methods provide a more accurate representation of material behavior and should be used for final design calculations. In the regression based methods, a nonlinear regression routine (Levenberg Marquardt) is used to vary the two model parameters (ε_o and σ_o) until the differences between model and test data are minimized. Results are shown in Figure 13. The average difference between model and test data is 1.2% of ε_o.[7]

Concluding Remarks

The constitutive model presented in this paper enables the performance predictions made in this paper's introduction. However, the full worth of the model not so limited. General structural analyses of spacecraft are often performed using the finite element method. Key to the method is selection of a proper material constitutive model. Previous to the crease model, the effects of random material wrinkles were difficult to included in a general structural analysis because a viable wrinkled thin film constitutive model did not exist.

This paper presents a general constitutive model that enables the elastic analysis of arbitrary wrinkled thin film structures. The model should be implemented as a hyperelastic material or as a specialization of a hypoelastic material model. This capability is typically included in commercial finite element analysis codes through the definition of user defined hyperelastic or hypoelastic materials. Predefined hyperelastic models such as the Odgen and Mooney-Rivlin formulations were developed for rubber and may not have the dexterity to represent wrinkled thin films. Due to their similar deformation mechanisms, it is likely that predefined hyperelastic foam models are better suited to representing wrinkled thin film behavior.

References

1 Freeland, R. E., Bilyeu, G. D., Veal, G. R., and Mikulas, M. M., "Inflatable Deployable Space Structures Technology Summary," *Proceedings of the 49th International Astronautical Congress*, Sept. 28-Oct. 2, 1998, Melbourne, Australia, IAF-98-I.5.01.

2 Freeland, R. E., Bilyeu, G. D., Veal, G. R., Steiner, M. D., and Carson, D. E., "Large Inflatable Deployable Antenna Flight Experiment Results," *Proceedings of the 48th Congress of the International Astronautical Federation*, October 6-10, 1997, Turin, Italy.

3 Murphey, T. W. and Mikulas, M. M., Jr., "Nonlinear Effects of Material Wrinkles on the Stiffness of Thin Polymer Films," *Proceedings of the 40th AIAA/ASME/ASCE/AHS/ASC Structures, Structural Dynamics, and Materials Conference and Exhibit*, April 12-15, 1999, St. Louis, MO., AIAA 99-1341.

4 Calladine, C. R.. *Theory of Shell Structures.* Cambridge University Press, 1983.

5 Timoshenko, S. P. and Gere, J.M., *Theory of Elastic Stability*, 2nd edition, McGraw-Hill Publishing Company, 1961, pp. 28, pp. 32.

6 Lin, T. H., "Shortening of Column with Initial Curvature and Eccentricity and Its Influence on the Stress Distribution in Indeterminate Structures" *Proceedings of the 1st National Congress on Applied Mechanics*, ASME, New York, 1952.

7 Murphey, T. W., "A Nonlinear Elastic Constitutive Model for Wrinkled Thin Films" Ph. D. Disseration, University of Colorado at Boulder, 2000.

Figure 1: The profile of wrinkles with amplitude of 0.0078 in and wavelength of 0.5 in.

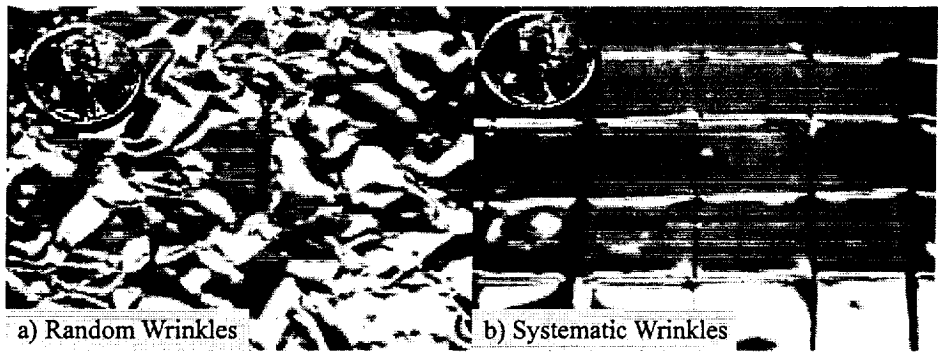

Figure 2: Examples of random and systematic material wrinkles in unstressed thin film samples (0.5 *mil* Kapton® HN).

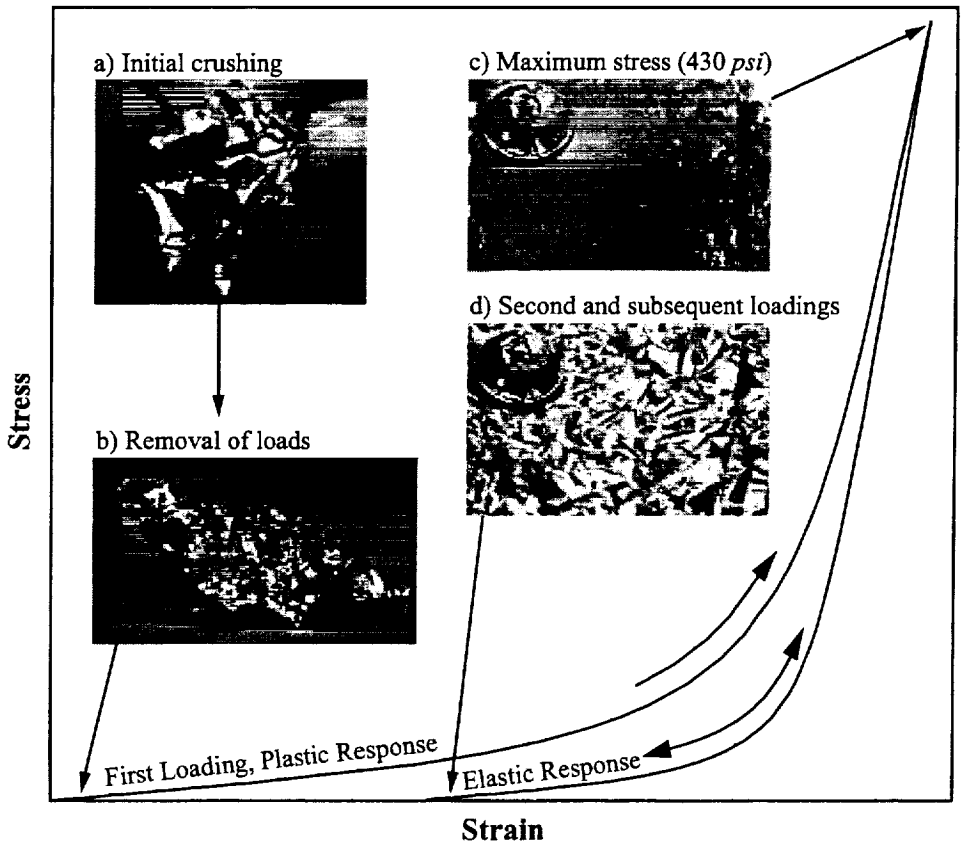

Figure 3: Plastic and elastic response load cases for wrinkled thin films.

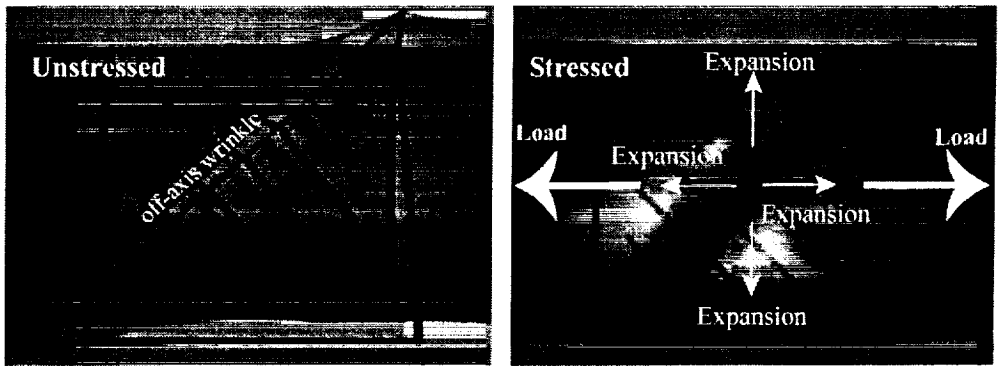

Figure 4: Off-axis wrinkle expansion causes a negative Poisson's ratio.

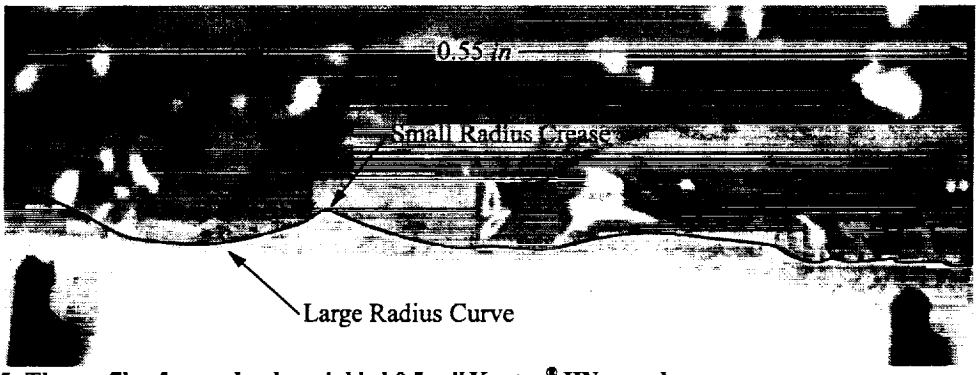

Figure 5: The profile of a randomly wrinkled 0.5 *mil* Kapton® HN sample.

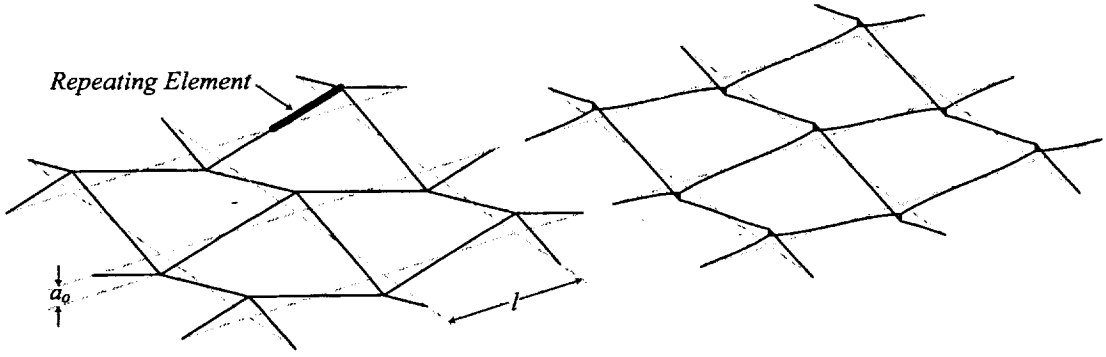

a) Undeformed Crease Model b) Deformed Crease Model ($\alpha_1 = 2$, $\alpha_2 = 0$)

Figure 6: The creased beam model (solid lines) shown in original and deformed configurations (dashed lines are not part of the model, they are to aid visualization).

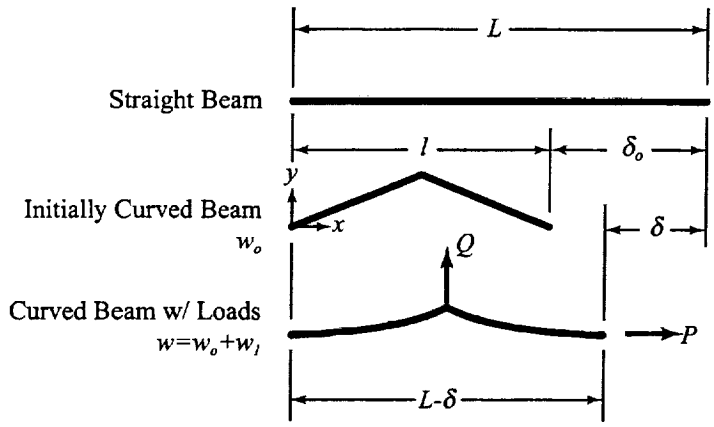

Figure 7: Repeating element analysis dimensions.

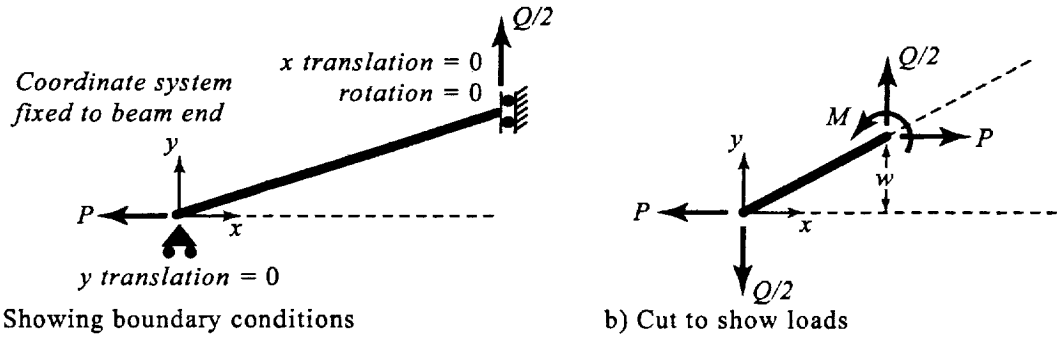

Figure 8: Free body diagram for model repeating element.

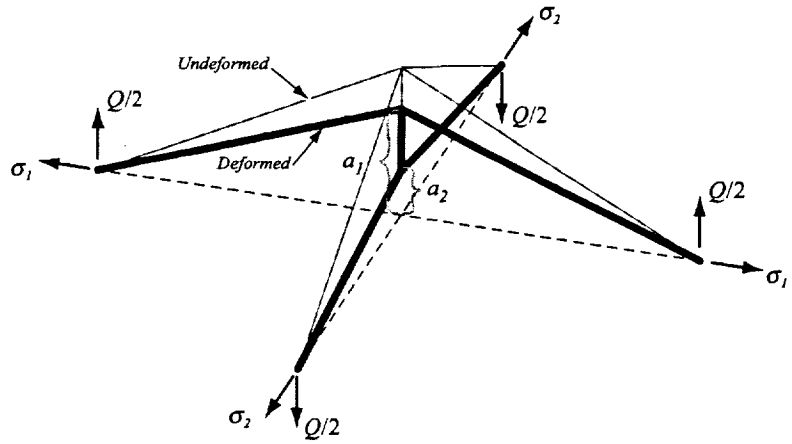

Figure 9: Force balance on crease model unit cell.

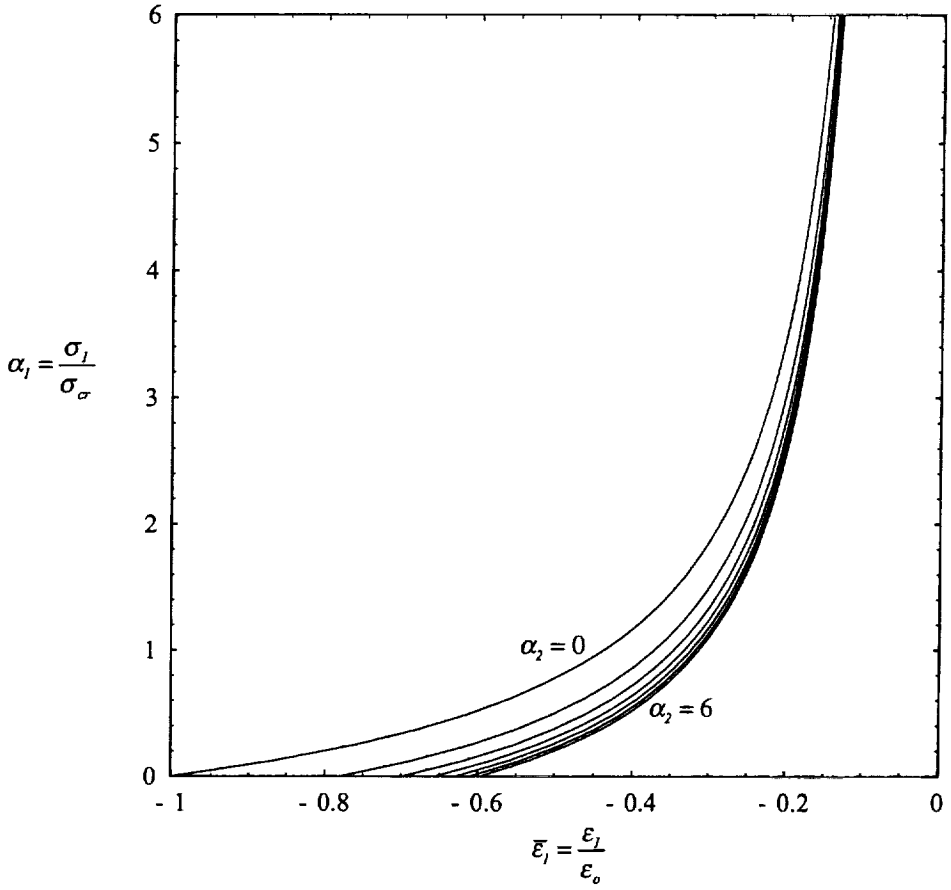

Figure 10: Constitutive behavior of crease model.

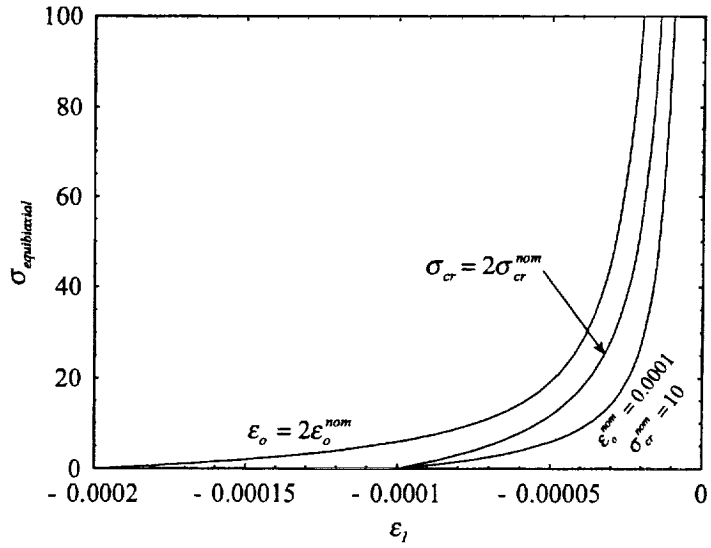

Figure 11: Equibiaxial stress-strain constitutive behavior of crease model.

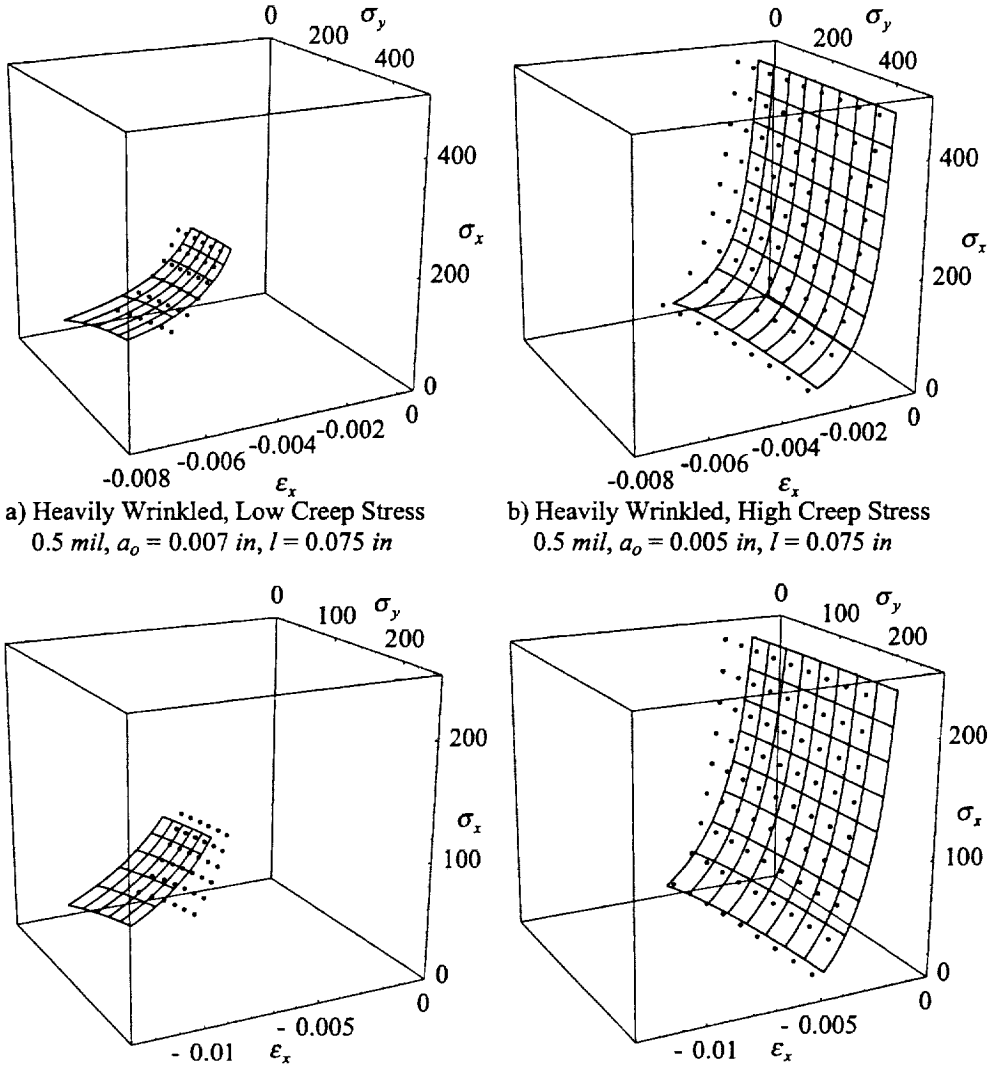

a) Heavily Wrinkled, Low Creep Stress
0.5 *mil*, $a_o = 0.007$ *in*, $l = 0.075$ *in*

b) Heavily Wrinkled, High Creep Stress
0.5 *mil*, $a_o = 0.005$ *in*, $l = 0.075$ *in*

c) Heavily Wrinkled, Low Creep Stress
1.0 *mil*, $a_o = 0.008$ *in*, $l = 0.094$ *in*

d) Heavily Wrinkled, High Creep Stress
1.0 *mil*, $a_o = 0.006$ *in*, $l = 0.094$ *in*

Figure 12: Biaxial tensile test data and model predictions based on directly measured model parameters (Kapton® Tab E). Dots represent test data and lines represent the model.

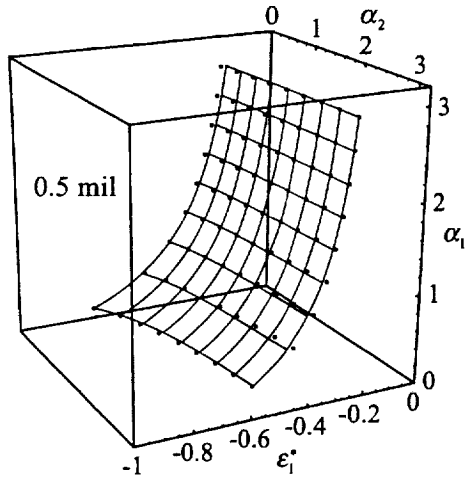

a) Moderately Wrinkled, High Creep Stress.

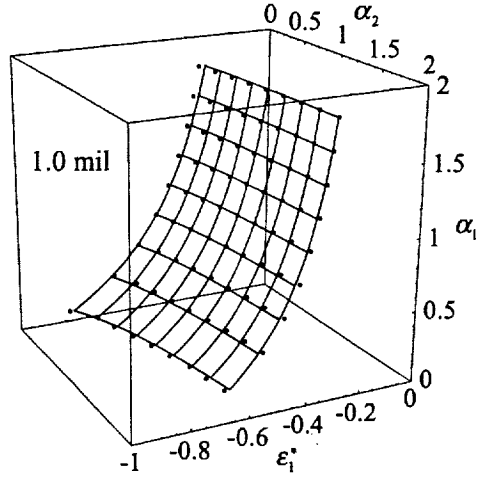

a) Moderately Wrinkled, High Creep Stress.

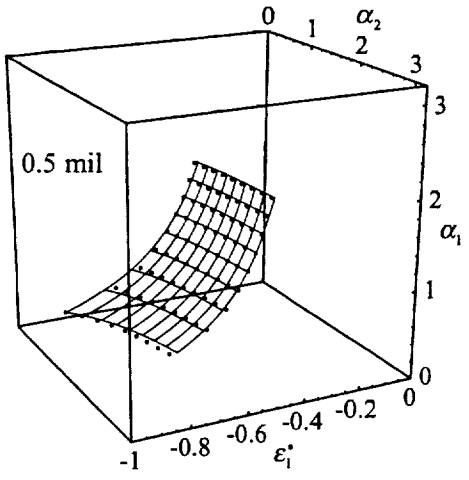

b) Heavily Wrinkled, High Creep Stress

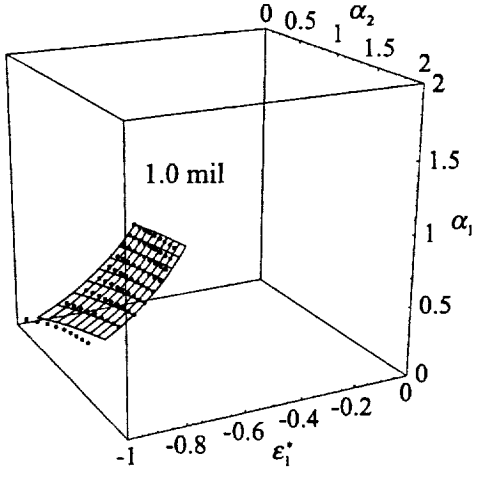

b) Heavily Wrinkled, High Creep Stress

Figure 13: Equibiaxial tensile test data and model predictions based on nonlinear regression parameter estimation method (Kapton® Tab E). Dots represent test data and lines represent the model.